Hui Zhang, Haijun Xue & Ningtao Mao (2018), The Journal of The Textile Institute,
DOI: 10.1080/00405000.2018.1429241

The disappearance of photocatalytic properties of titanium dioxide nanoparticles formed on PET fabrics treated in a simultaneous hydrothermal-dyeing process

Hui Zhang[a] Haijun Xue[a] Ningtao Mao[b]

a School of Textile Science and Engineering, Xi 'an Polytechnic University, Xi'an, China
b School of Design, University of Leeds, Leeds, UK

Received 04 Apr 2017; Accepted 15 Jan 2018

Abstract

In this paper, the influences of dyestuff Disperse Blue 79 and corresponding dyeing auxiliaries on the microstructure and the photocatalytic activities of titanium dioxide nanoparticles formed on polyethylene terephthalate (PET) fabric modified with tetrabutyl titanate in a simultaneous hydrothermal-dyeing process are studied. In contrast to the apparent photocatalytic activities of the crystalline titanium dioxide particles formed in the solely hydrothermal process using tetrabutyl titanate, the titanium dioxide nanoparticles formed in the simultaneous hydrothermal-dyeing process is non-crystalline and is covered with a layer of organic substances. It is thus concluded that the microstructure of the as-synthesized titanium oxide nanoparticles is greatly influenced by the presence of dyestuff and its corresponding dyeing auxiliaries. It is also found that these resultant non-crystalline titanium oxide nanoparticles in the simultaneous hydrothermal-dyeing process do not show any photocatalytic activity; the disappearance of the photocatalytic activity of the resultant titanium oxide nanoparticles in the simultaneous hydrothermal-dyeing process might be due to both their non-crystalline microstructure and their surface coating of organic substances.

Key words: photocatalytic, Disperse Blue 79 dye, tetrabutyl titanate, hydrothermal-dyeing process

1. Introduction

Anatase titanium dioxide ($Ti0_2$) is known as the most active photocatalyst with a strong

oxidative potential. It has been extensively utilized in a variety of textiles to shield ultraviolet (UV) rays, decompose organic compounds (Awitor, Rivaton, Gardette, Down, & Johnson, 2008; Ratova, West, & Kelly, 2014), and for achieving anti-bacterial polyester fibers (Li, Xu, Zhou, & Wang, 2010). Polyethylene terephthalate (PET) has been widely applied in the textile industry for its remarkable optical and mechanical properties, and it is usually colourized by disperse dye in the high temperature and high pressure conditions. PET fibers incorporating with TiO_2 nanoparticles have been produced via electrospinning technique (Deniz, Celebioglu, Kayaci, & Uyar, 2011). **In situ** growth of TiO_2 nanoparticles using TiO_2 precursor in hot water (Meng, Feng, Li, & Zhang, 2012), and TiO_2 supported PET sheet for photocatalytic oxidation of organic dye in sunlight have been investigated (EL-Mekkawi, Nady, Abdelwahab, Mohamed, & Abdel-Mottaleb, 2016). The $Ti0_2$-coated PET fabrics have been prepared via hydrothermal process using tetrabutyl titanate (Zhang, Xu, & Yang, 2011) while their photocatalytic activities have not been investigated. The photocatalytic leroperties of TiO_2 nanoparticles on PET fabrics treated in hydrothermal process using titanium sulfate and urea aqueous solutions (Zhang, Zhu, & Sun, 2012) have also been studied, however, the photocatalytic properties of TiO_2 nanoparticles on PET fabrics treated in a simultaneous hydrothermal-dyeing process have never been investigated.

However, the mechanical and thermal properties of PET fibers containing titanium oxide are usually degraded upon exposure to UV or visible light radiation for a long time, which is caused by the rupture of covalent bonds initiating photolytic (without intervention of oxygen) and photo-oxidative (fixation of oxygen) reactions; the color yield of PET yarn containing titanium oxide can be distinctly influenced by the amount of titanium oxide particles within fibers (Cho, 2004), and the photocatalytic decolorization and mineralization of reactive dyes by TiO_2 nanoparticles loaded on PET fabrics have been reported (Ghoreishian, Badii, Norouzi, & Malek, 2016; Ghoreishian et al., 2014). In addition, the adhesion between TiO_2 film and PET substrate can be effectively enhanced by applying commercial TiO_2 powders with a little amount hydrothermal TiO_2 cement as connection agent (Zhang, Wu, et al., 2012). Recently, both colorant-free dyeing and hydrophilic modification of PET fabric have been synchronously carried out sing hydrogen peroxide in the presence of nano TiO_2 under UV irradiation (Zhang, Liang, & Zhang, 2016).

In this paper, we intend to form a layer of TiO_2 on the surface of dyed PET fabrics to absorb UV light to provide a barrier against the photo-fading of disperse dye and reduce the photo-

oxidative degradation of dyed PET fabric. PET fabrics are treated and dyed in hydrothermal process using a suspension containing Disperse Blue 79 dye and tetrabutyl titanate aqueous solution. The photocatalytic activity of TiO_2 coating and self-cleaning performance of the resultant PET fabric are investigated. The fabric properties such as tensile, optical, color fastness to UV light, and capillary effect as well as the percentage of exhaustion of Disperse Blue 79 dye are also examined. The changes of the photocatalytic activities of PET fabrics are analyzed in relation to the changes of the microstructure, morphology, chemical composition, surface binding state of the as-synthesized titanium dioxide articles on PET fabrics, which are characterized by field emission scanning electron microscopy (FESEM), energy dispersive X-ray spectroscopy (EDX), X-ray diffraction (XRD), transmission electron microscopy (TEM), and X-ray photoelectron spectroscopy (XPS) techniques.

2. Experimental section

2.1. Materials and reagents

The gray PET fabric was friendly provided by the Northwest No.5 Textile Mill. The linear densities of both warp and weft yarns were identical (12.3 tex). The yarn densities in warp and weft directions were 113 and 88 ends per 10 cm, respectively. The fabric mass per unit area was 115 gram per square meter. The chemical agents used in this experiment were all analytical reagent grade, including sodium hydroxide (NaOH), ammonium dihydrogen phosphate ($NH_4H_2PO_4$), ethanol (CH_3CH_2OH), acetone (CH_3COCH_3), sodium carbonate ($NaCO_3$), tetrabutyl titanate ($C_{16}H_{36}0_4Ti$), methyl orange (MO, $C_{14}11_{15}N_3Na0_3S$) dye. The Disperse Blue 79 (CAS No.12239-34-8, $C_{24}H_{27}BrN_6O_{10}$) dye and dispersing agent NNO (CAS No.36290-04-7, $C_{21}H_{14}Na_20_6S_2$) were obtained from a local printing and dyeing mill. The deionized water was used throughout this experiment.

2.2. Pretreatment of PET fabrics

To generate the polar/hydrophilic groups on PET fabric surface (Hashemizad, Montazer, & Rashidi, 2012), a certain amount of gray PET fabric with a size of 30 x 30 cm^2 was first treated with 10 g/L of sodium hydroxide solution at a temperature of 85 °C for 40 min according to a material to liquor ratio of 1:50, and was then washed repeatedly with deionized water until the pH of the solution was neutral, and was finally dried in an

oven. The base deweighting rate of PET fabric was about 7.6% after being etched by alkali, and the fabric shrinkages for both warp and weft directions were the same 2.3%.

2.3. Dyeing of PET fabrics

The PET fabric was dyed using the high temperature and high pressure dyeing method at a stirring rate of 200 rpm. The dye concentration of Disperse Blue 79 was applied to 1% (o.w.f, on weight the fabric). The liquor ratio of the weight of fabric in relative to the volume of dyeing liquor was 1:60. About 2 g/L of ammonium dihydrogen phosphate and 1 g/L of dispersing agent NNO were first added into the dye bath. The PET fabric sample was then put into the dye bath at 30 °C for 5 min. The dye bath was subsequently heated to 130 °C at a heating rate of 1 °C per minute, and was kept for 60 min at the same temperature. After that, the dye bath was cooled down to 50 °C with cool water in 60 min. During dyeing rocess, about 3 mL of dyeing liquor was extracted from the dye bath at certain time intervals, and the absorbance at the maximum absorption wavelength of 526 nm was immediately measured using a VIS-7220 N spectrophotometer (Beijing Rayleigh Analytical Instrument Corp.). The percentage of exhaustion E (%) was calculated on the basis of formula (1):

$$E(\%) = \left(1 - \frac{A_t}{A_0}\right) \times 100\% \qquad (1)$$

where A_o was the absorbance of initial dyeing liquor without adding the fabric sample, A_t was the absorbance of dyeing liquor with the fabric sample at time t. The average of percentage of exhaustion for the dyed PET fabric was given after three measurements.

The dyed PET fabric was treated with a mixture solution containing 2 g/L of soap and 2 g/L of sodium carbonate at 85 °C at a liquor ratio of 1:30 for 15 min. Lastly, the PET fabric was washed with cold water and dried at 60 °C. In comparison with the pretreated PET fabric, the shrinkages of the dyed PET fabric were 8.2 and 4.8% in warp and weft directions, respectively.

2.4. Immobilization of TiO_2 on PET fabrics

Similar to previous research (Zhang et al., 2011), the immobilization of TiO_2 on PET fabric was realized by a hydrothermal method. Five milliliter of tetrabutyl titanate was first added into 50 mL of ethanol solution under vigorous stirring. After 10 min, 50 mL of 95% (wt.%) ethanol solution was then added under continuous stirring. The mixture

solution was finally diluted to 1 L with deionized water. The liquor ratio of pretreated PET fabric to tetrabutyl titanate precursor solution was 1:60. The precursor solution of tetrabutyl titanate combined with the pretreated PET fabric was heated to 130 °C at a heating rate of 1 °C per minute and at a speed of 200 rpm. After 120 min of reaction at 130 °C, the mixture solution was cooled down to 50 °C with cool water in 60 min. The TiO_2 coated PET fabric was successively washed with acetone, anhydrous ethanol, and deionized water at room temperature for 15 min, respectively. The as-synthesized powder remaining in the solution, which was denoted as P1, was collected by centrifugation, andrepeatedly washed with acetone, anhydrous ethanol, and deionized water, respectively, and finally dried in an oven at 120 °C.

2.5. Simultaneous hydrothermal-dyeing treatment of PET fabrics

The precursor solution of tetrabutyl titanate was first prepared according to the procedure mentioned in section 2.4. A certain amount of Disperse Blue 79 dye was then added into the precursor solution to maintain the concentration of dye o.w.f 1% under continuous stirring, followed by the addition of 2 g/L of ammonium dihydrogen phosphate and 1 g/L of dispersing agent NNO. The PET fabric was subsequently immersed in the mixed suspension for 10 min, which was heated to 130 °C at a heating rate of 1 °C per minute and at a speed of 200 rpm. After 30, 60, and 120 min of reaction at 130 °C, respectively, the suspensions were cooled down to 50 °C with cool water within 60 min. The corresponding resultant PET fabrics were denoted as H30, H60, and H120. The fabric samples were soaped with aqueous solution composed of 2 g/L of soap and 2 g/L of sodium carbonate at 85 °C at a liquor ratio of 1:30 for 15 min, and then washed with acetone, anhydrous ethanol, and deionized water at room temperature for 15 min, respectively. During the hydrothermal treatment, about 3 mL of mixture solution was extracted from the suspension and then centrifugated to remove the particles; thus the percentage of exhaustion was calculated using the above formula ( ) by measuring the absorbance of dyeing liquor. The remained powder was also collected via centrifugation and washed with acetone, anhydrous ethanol, and deionized water, respectively, and finally dried at 120 °C. The as-synthesized I*owders corresponding to the H30, H60, and H120 fabric samples were denoted as P30, P60, and P120, respectively. The shrinkages of the H60 fabric are 7.4% in warp direction and 4.4% in weft direction compared with the pretreated

PET fabric.

2.6. Characterization techniques

The surface morphology of PET fabric was observed using a ZEISS EVO18 FESEM. EDX analysis was also performed by an Oxford INCA Energy 350 EDX system attached to the FESEM.

The crystal structure of the as-synthesized powder was analyzed using a 7000S XRD spectroscopy diffractometer equipped with Cu Ka_i radiation (λ=0.154056 nm, 40 kV and 40 mA) at a scan step of 0.02º and a scan rate of 5º per minute. The microstructure of the as-synthesized powder was investigated using TEM (JEOL3010, 200 keV). The surface chemical bonding states of PET fabric were determined by a XPS (AXISULTRA, Kratos, U.K). The XPS spectra were recorded with monochromatic Al Ka (1486.71 eV) line at a power of 100 W (10 mA, 10 kV) with the vacuum about 10^{-8} Torr. The charge neutralizer was used to compensate for surface charge effects, and binding energies were calibrated using the C_{1s} hydrocarbon peak at 284.8 eV.

2.7. Measurement of fabric properties

The PET fabric samples were preconditioned prior to testing in a standard environment according to IS0139:2005. The photocatalytic activities of PET fabrics and as-synthesized powders were performed by monitoring the degradation of MO dye at 10 °C under UV and visible light irradiations, respectively. A piece of PET fabric with a size of 7 x 7 cm^2 (or 0.01 g of as-synthesized powder) was immersed in 5 mg/L of 50 mL MO aqueous solution. After reaching the adsorption and desorption equilibrium, the testing solution was irradiated by a 500 W Xeon lamp at a distance of 8 cm. For UV light irradiation, a series of visible light filters was used to block off visible light. In contrast, the 400 nm cut-off UV filters were used to simulate the visible light irradiation. Five milliliter of MO solution was centrifuged at 12,000 rpm for 10 min to obtain the supernatant. The absorbance of the extracted supernatant at the maximum absorption wavelength 464 nm was measured using the VIS-7220 N spectrophotometer every hour. The degradation rate D was calculated according to the formula (2).

$$D = (1 - \frac{B_t}{B_0}) \times 100\% \qquad (2)$$

Where B_0 was the initial absorbance of MO solution which reached the absorption

equilibrium, and B_t was the absorbance of MO solution at time t.

The self-cleaning performance was tested by observing the decoloration of MO dye stained on PET fabric. A certain size of 4×4 cm^2 PET fabric was immersed in 100 mg/L of 50 mL MO aqueous solution at 15°C for 10 min and dried at 80°C. The dipping was repeated for three times. The stained PET fabric was then irradiated by a 500 W metal halide lamp, which was simulated to sunlight with an illumination of 6.0×10^3 lux determined by a TES-1332 digital light meter. The optical pictures were photographed using a Samsung ST700 digital camera every hour.

The tensile properties of PET fabric were carried out on a YG(B)026D-500 tensile tester according to ISO13934-1:1999. The gauge length was 200 mm and the fabric width was 50 mm. The constant rate of extension was 100 mm/min and the pretension was 2 N.

To clarify the influence of TiO_2 coating on the stain colour, the dyed PET fabric was exposed to three Philips UV lamps (3×20 W, main wavelength 254 nm) with a radiation intensity of 3.92 $mW\cdot cm^{-2}$ determined by a ST-12 UV illumination meter. The colour fastness to ultraviolet light of dyed fabric was assessed by measuring the colour yield (K/S value) at the maximum absorption wavelength 526 nm. The change of K/S value was recorded every 24 h using a SF300 Plus colorimeter (Datacolor Inc.) under D65/10° illuminant. The colorimeter was calibrated before testing against a standard white board. The K/S value was calculated according to Kubelka–Munk equation (3).

$$K/S = \frac{(1-R)^2}{2R} \qquad (3)$$

Where K and S were the coefficients of absorption and scattering respectively, and R was the diffuse reflectance of dyed PET fabric.

The diffuse reflectance spectrum (DRS) of PET fabric was obtained using a PE LAMBDA 950 UV-VIS-NIR spectrophotometer equipped with a 150 mm integrating sphere at a scan rate of 120 nm per minute over the wavelength 200–800 nm.

The wicking effect of PET fabric was measured by reference the standard FZT01071-2008 ‘Textiles-Test Method for Capillary Effect’. The deionized water was used for recording the liquor wicking height at 21°C at certain time intervals. The width of fabric was set at 3 cm and the average of three measurements was given.

3 Results and Discussion

3.1 TiO_2 nanoparticle film deposited on the surface of PET fabrics

FESEM images of the surfaces of solely dyed, simultaneous hydrothermal-dyeing treated, and TiO_2 coated PET fabrics are shown in Figure 1.

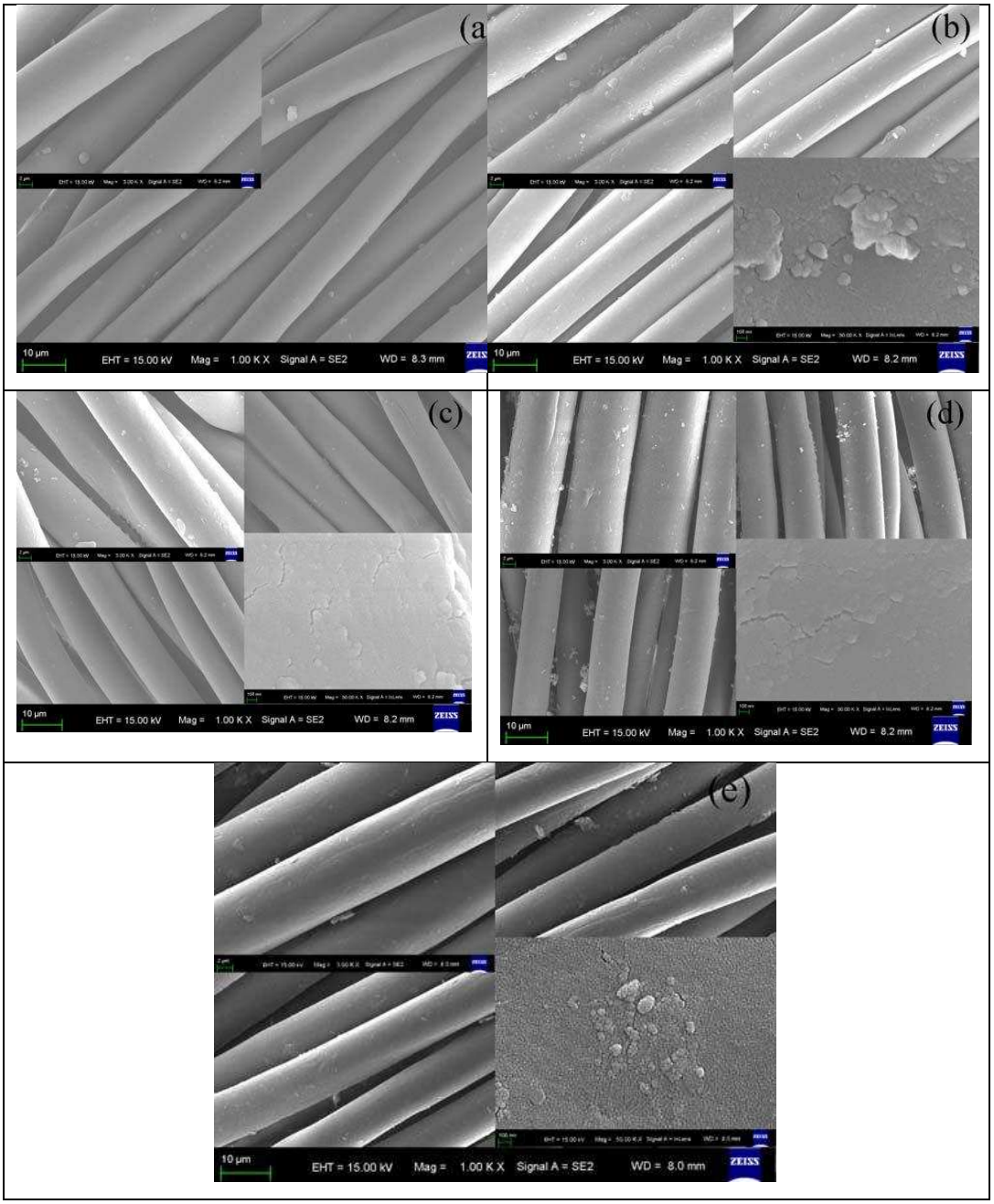

Figure 1. FESEM images of PET fabrics: (a) Solely dyed with Disperse Blue 79; Simultaneous hydrothermal-dyeing treatments for (b) H30, (c) H60 and (d) H120 samples; (e) TiO_2 coated

When the PET fabric is solely dyed with Disperse Blue 79 [Fig. 1(a)], the surfaces of PET fibers are coated with a continuous layer of fine particulate substances, which are caused by the dyeing processing. For PET fabrics dyed and hydrothermal treated in one step [Fig. 1(b), 1(c) and 1(d)], there is little difference in the fiber surface morphologies among PET fabric

samples H30, H60 and H120. The fiber surfaces are coated with some large agglomerates and a layer of granulated TiO_2 nanoparticles, and these granulates are composed of tiny particles less than 100 nm in particle sizes, which are confirmed by the high-resolution FESEM image as illustrated in the corresponding lower right corner. For PET fabrics treated solely with tetrabutyl titanate in hydrothermal process [Fig. 1(e)], the fiber surfaces are deposited with a film of particulates consisting of nanometer-sized particles. The nanoparticles on the TiO_2 coated PET fabrics are more clearly observed than those on the simultaneous hydrothermal-dyeing treated ones.

Whether the above nano-sized particles coated on the surface of PET fabrics contain any TiO_2 particles are decided primarily by using EDX elemental analysis. The approximation of chemical compositions of the coating layer on the surface PET fabrics are quantified using EDX spectra, as displayed in Figure 2. Only the two elements, carbon (C) and oxygen (O), are observed on the surface of PET fabrics solely dyed with Disperse Blue 79, their atom percentages are 70.25% and 29.75% respectively [Fig. 2(a)]. The elements of S and Na from dispersion agent NNO are not found either, and this indicates that element Na might be washed off and the trace amount of S might be beyond the detection limit of the EDX device, nevertheless the elements of C and O from organic substances are clearly identified. For the fabric sample (e.g., H60) treated in a simultaneous hydrothermal-dyeing process, a small atom percentage of the element Titanium (Ti) (0.04%), together with the elements of C (70.61%) and O (29.35%), is detected, suggesting the existence of titanium oxide [Fig. 2(b)]. A slightly greater percentage of element Ti (0.12%), as well as C (71.63%) and O (28.25%) is detected in the TiO_2 coated PET fabrics [Fig. 2(c)]. In comparison with the fabric sample H60, the amount of Ti element in the TiO_2 coated PET fabric samples from solely hydrothermal process is much greater. It is thus envisaged that the existences of disperse dye and dyeing auxiliaries in the reaction solution may have affected the formation and deposition of TiO_2 particles on PET fabrics.

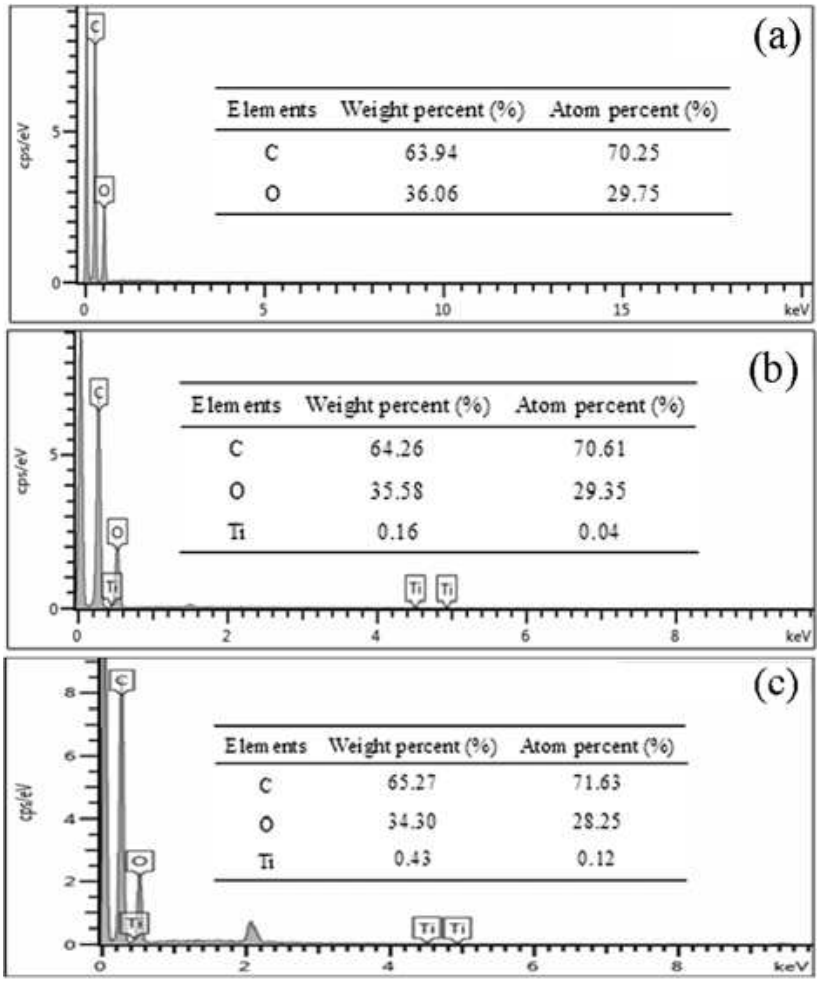

Figure 2. EDX spectra of PET fabrics: (a) Solely dyed with Disperse Blue 79; (b) Simultaneous hydrothermal-dyeing treatment for H60 sample; (c) TiO_2 coated fabrics from solely hydrothermal treatment

3.2 Microstructure of TiO_2 particles formed on the surface of PET fabrics

The phase structure of as-synthesized particles from the residual hydrothermal solutions rather than the particles deposited on PET fabrics were analyzed using XRD techniques, because the amount of these particles deposited on PET fabric is beyond the detection limit of XRD instrument. XRD patterns of the as-synthesized particles are presented in Figure 3. A series of characteristic peaks at 2θ of 25°, 38°, 48°, 54°, 55°, 63°, and 75° in the XRD pattern of the powder P1 are observed. These diffraction peaks are in accord with {101}, {004}, {200}, {105}, {211}, {204}, and {215} planes of tetragonal anatase TiO_2 (JCPDS card No.21-1272) (Yang, & Zeng, 2004). The result indicates that the nanoparticles coated on PET fabrics using tetrabutyl titanate under hydrothermal conditions are ascribed to anatase TiO_2. However, the characteristic diffraction peaks of anatase TiO_2 are not found in the XRD

patterns of the nanoparticles from P30, P60 and P120 powders obtained in a simultaneous hydrothermal-dyeing process while a broad diffraction peak centered at around 2θ=30° is noticed, suggesting that the amorphous or non-crystalline TiO_2 nanoparticle film are formed on PET fabric samples H30, H60, and H120. Hence, the hydrothermal and dyeing time duration at 130°C has no effect on the phase structure of TiO_2 nanoparticles. While Disperse Blue 79 dyestuff does not dissolve in water, the soluble dyeing auxiliaries, such as ammonium dihydrogen phosphate and dispersing agent NNO, adsorbed on the surface of TiO_2 particles may prevent the crystallization of anatase from amorphous TiO_2 (Yu, et al, 2007).

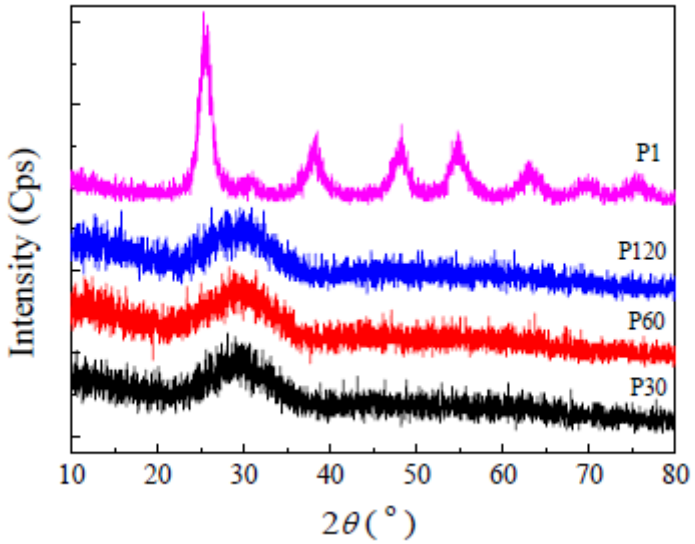

Figure 3. XRD patterns of the as-synthesized TiO_2 particles collected from remaining powders in hydrothermal solutions

The microstructure of the powder P60 is further characterized by TEM analysis. The TEM, high-resolution TEM, and selected area electron diffraction (SAED) are represented in Figure 4. It is evident that the spherical submicrometer-sized particles of powder P60 is constituted with nanoparticles smaller than 20 nm in average particle size [Fig. 11(a) and 11(b)]. The peripheral surfaces of these nanoparticles are obscure and might be covered with a thin film of other materials. Furthermore, the crystallite lattice of as-synthesized nanoparticle is not observed in the high-resolution TEM image [Fig. 11(c)]. This is confirmed by the SAED pattern without any diffraction rings [Fig. 11(d)]. Therefore, the as-synthesized nanoparticles coated on PET fabric are not crystallised during the simultaneous hydrothermal-dyeing process.

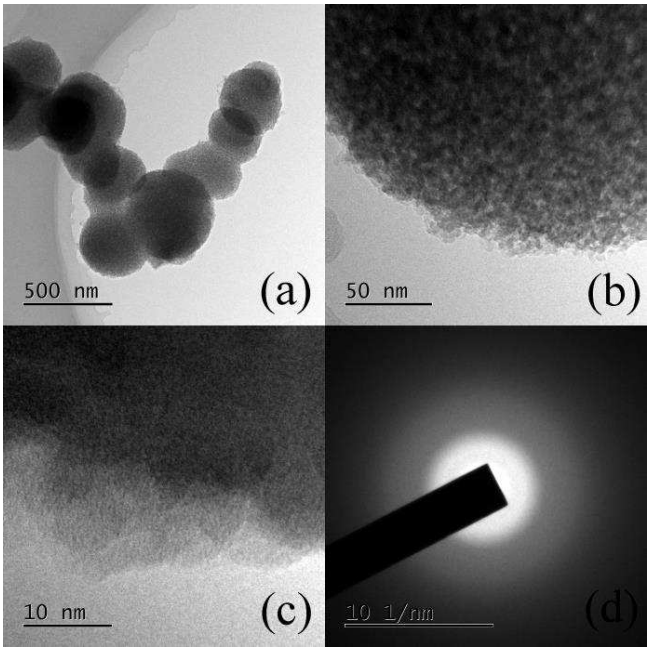

Figure 4. TEM (a) and (b), HRTEM (c) and SAED pattern (d) of the powder P60

Further analysis of the TiO_2 particles existed on the surface of PET fabrics are studied by using XPS survey spectra. C_{1s}, O_{1s} and Ti_{2p} core-level deconvolution spectra of the TiO_2 coated PET fabrics (H1) and simultaneous hydrothermal-dyeing treated PET fabrics (e.g., H60) are compared in Figure 5. The quantitative elemental analysis is given in Table 1. It is apparent that, besides the elements of C_{1s} and O_{1s}, the Ti_{2p} element is identified in the XPS survey spectrum of the TiO_2 coated PET fabrics. However, the Ti_{2p} element is not found in the simultaneous hydrothermal-dyeing treated PET fabrics, H60. This is because the effective detecting depth for XPS surface analysis instrument is less than 10 nm, implying that the outer layer of TiO_2 nanoparticle formed during hydrothermal process is almost covered by a layer of organic substances with a certain thickness (The elements of S and Na from dispersion agent NNO are not shown either, and this indicates that element Na might be washed off and the trace amount of S might be beyond the detection limit of the EDX device, nevertheless the elements of C_{1s} and O_{1s} from organic substances are clearly identified.). So the photoactivity of PET fabric H60 could be lost (see section 3.3). For the high-resolution Ti_{2p} XPS spectrum of the TiO_2 coated PET fabrics from solely hydrothermal process without dispersion dye, it can be deconvoluted into four distinct sub-peaks. The sub-peaks at 458.66 eV and 464.36 eV are attributed to $Ti^{4+}{}_{2p3/2}$ and $Ti^{4+}{}_{2p1/2}$ of TiO_2 nanoparticle, respectively; The sub-peaks at 460.87 eV and 465.86 eV are ascribed to $Ti^{3+}{}_{2p3/2}$ and $Ti^{3+}{}_{2p1/2}$ respectively (Pandiyaraj et al, 2014), indicating the binding of Ti atoms of TiO_2 nanoparticle with O atoms of PET fabric (Zhang et al, 2011).

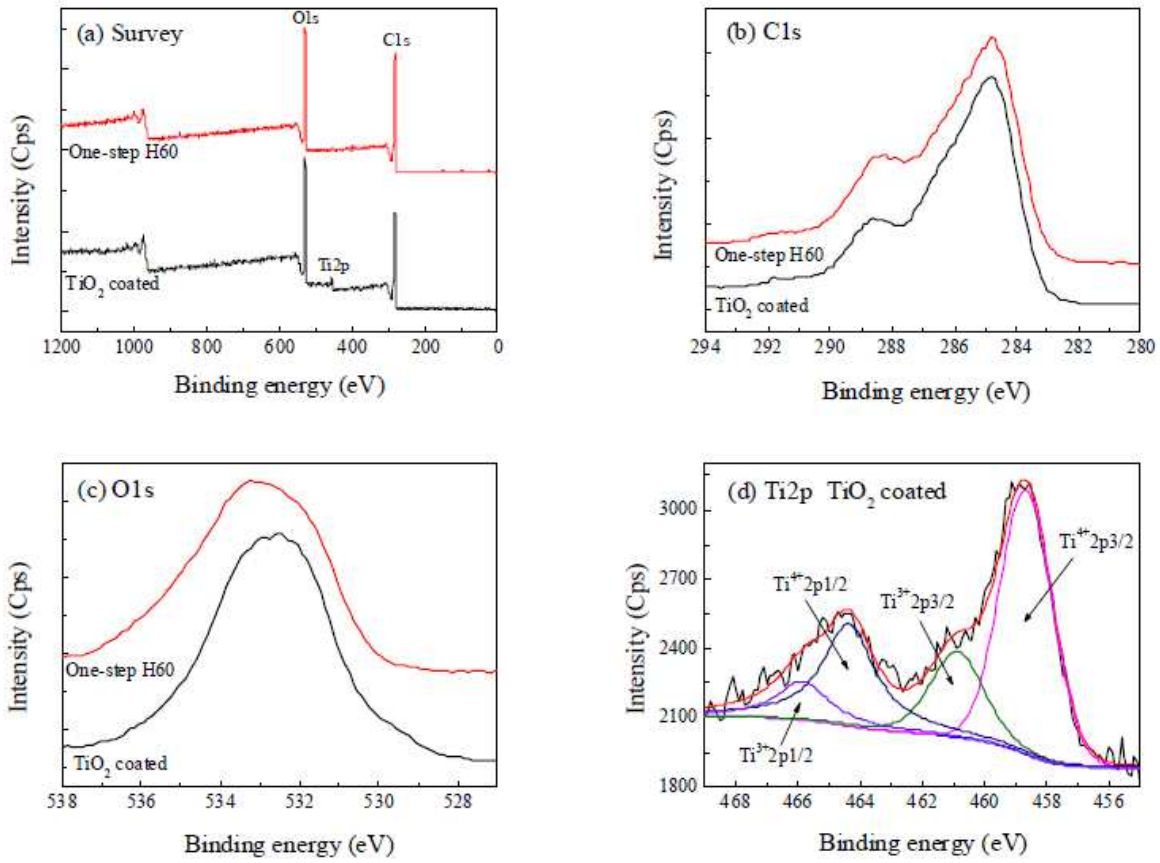

Figure 5. XPS (a) survey spectra and (b) C_{1s}, (c) O_{1s} and (d) Ti_{2p} core-level deconvolution spectra of TiO_2 coated and simultaneous hydrothermal-dyeing treated H60 PET fabrics

Table 1. The results of XPS elemental analysis of TiO_2 coated and simultaneous hydrothermal-dyeing treated H60 PET fabrics

PET fabrics	Peak	Binding energy (eV)	FWHM (eV)	Area (CPS·eV)	Atomic concentration (%)
TiO_2 coated	C1s	284.80	1.799	36527.2	71.58
	O1s	527.88	2.837	42601.0	27.39
	Ti2p	458.78	2.195	3966.0	1.03
One-step	C1s	284.80	1.825	39392.0	74.76
H60	O1s	529.60	1.832	39215.2	25.24

3.3 Photocatalysis and self-cleaning performance of hydrothermal treated PET fabrics

Photocatalysis effect of PET fabrics and as-synthesized TiO_2 powders is characterized as the degradation rates of organic MO dye solution under UV or visible light irradiation as shown in Figure 6. It is noted that the TiO_2 coated PET fabric and P1 powder have the photocatalytic

activities for the degradation of organic MO dye exposure to both UV and visible light irradiations. The degradation rate of MO solution increases gradually with the increase of time duration of exposure to irradiation. The P1 powder behaviours much better than the TiO_2 coated fabric. This is because the amount of TiO_2 nanoparticles in the P1 powder is much more than that in the TiO_2 coated fabric. After 6 hours of irradiation under UV and visible light irradiations, about 95% and 7.3% of MO dye are photo-degraded for the TiO_2 coated PET fabric respectively. Regarding to the P1 powder, about 95% and 31.3% of MO dye are photo-degraded after 4 and 6 hours of irradiation under UV and visible light irradiations respectively. It is known that a photon having energy greater than the band gap of TiO_2 generates an electron–hole pair when exposure to UV or visible light irradiation. The positive hole in the valence band can react with the absorbed water to produce H^+ and $\cdot OH$ radicals, and the electron in the conduction band can reduce oxygen to produce $O_2\cdot^-$ anions. Both hydroxyl radicals and peroxide anions are extremely reactive species, thus they can oxidize the organic compounds of MO dye until complete mineralization is achieved (Peng et al, 2012). However, the other PET fabrics including the fabrics treated in a simultaneous hydrothermal-dyeing process as well as the P60 powder do not show the capability of effective photo-degradation of MO dye solutions, although the simultaneous hydrothermal-dyeing treated PET fabrics (e.g., H60) is coated with a layer of TiO_2 nanoparticles which are not crystallised TiO_2 particles. As amorphous TiO_2 nanoparticles have been proved to have photocatalytic activities (Benmami et al, 2006; Zou et al, 2010; Kaur, & Singh, 2012; Sun et al, 2014), the lack of photocatalysis and self-cleaning performance in the resultant PET fabrics and P60 powder might be a result of the coating layer of organic dispersion agents, dyes and other additives from commercial dyestuff deposited on the surface of the TiO_2 nanoparticles.

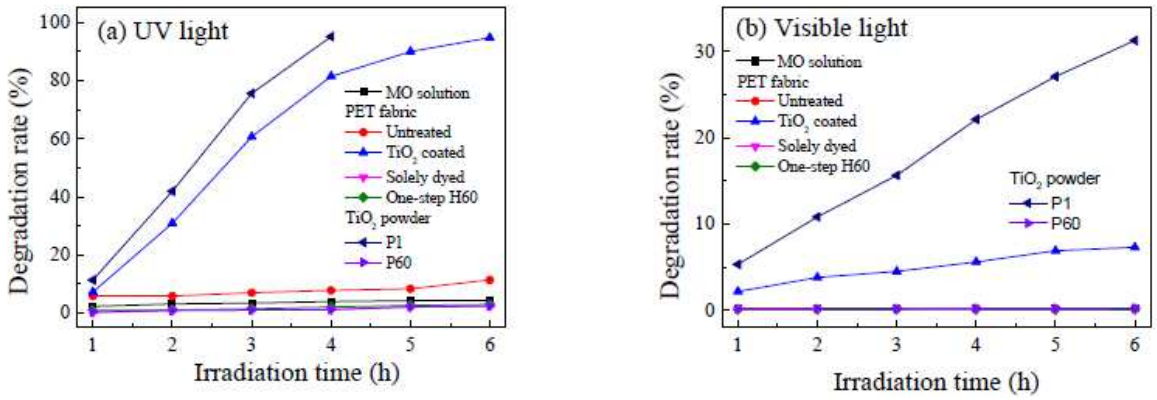

Figure 6. The degradation rate of MO solution irradiated by (a) UV and (b) visible lights

The self-cleaning effects of untreated, TiO_2 coated, solely dyed and simultaneous

hydrothermal-dyeing treated H60 PET fabrics stained by MO dye exposed to simulated sunlight irradiation at different times are shown in Figure 7. It is seen that the colours of the untreated, solely dyed and simultaneous hydrothermal-dyeing treated H60 PET fabrics have no distinct change with the increase of irradiation time. The K/S values of the solely dyed and simultaneous hydrothermal-dyeing treated H60 PET fabrics have no obvious change either. But for the TiO_2 coated PET fabrics, the intensity of shallow orange colour is gradually discoloured with increasing the irradiation time. After 5 h of irradiation, the fabrics are almost completely discoloured. It has been demonstrated that the electron-hole pair reacts with water to produce radical groups with strong oxidizability, which can further oxidize organic compounds to finally produce carbon dioxide and water (Rehan et al, 2013).

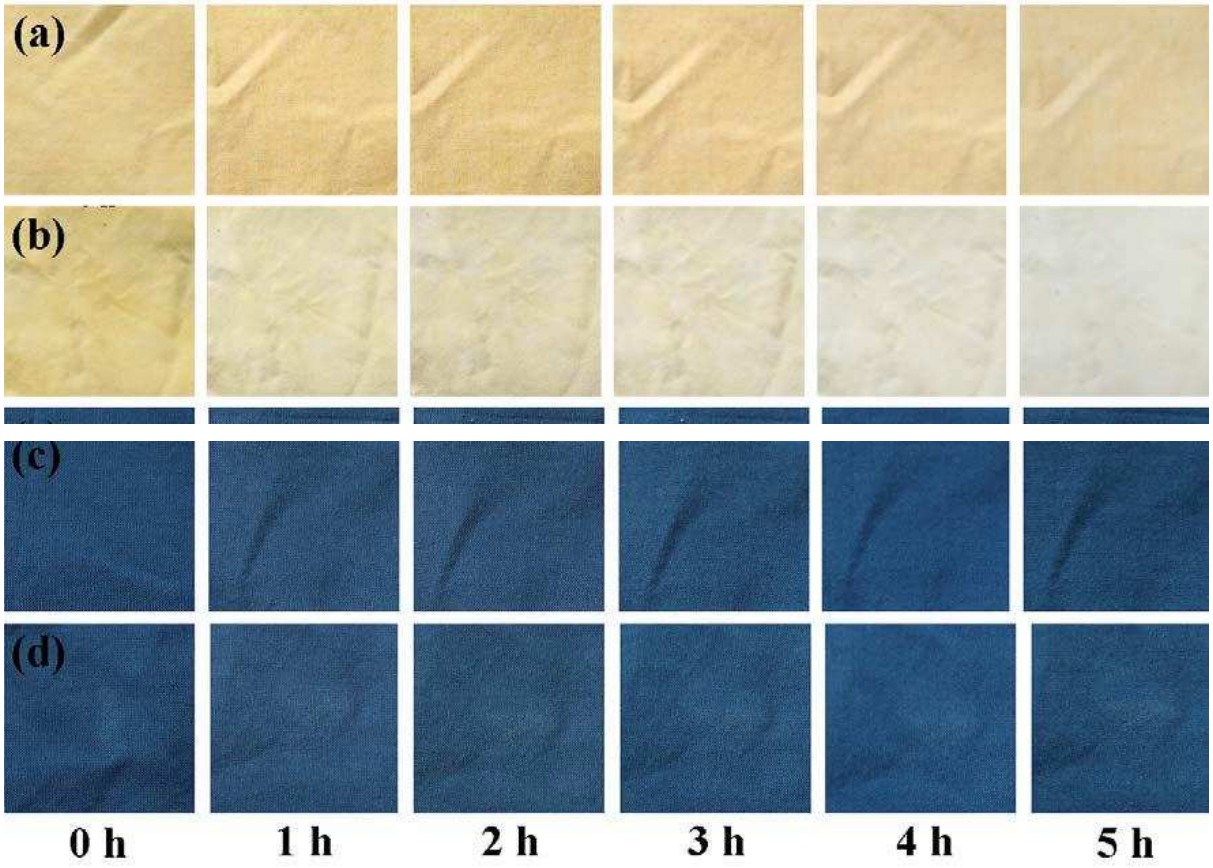

Figure 7. The self-cleaning effects of (a) untreated, (b) TiO_2 coated, (c) solely dyed and (d) simultaneous hydrothermal-dyeing treated H60 PET fabrics exposed to simulated sunlight irradiation at different times

3.4 Changes of other fabric properties

3.4.1 Tensile Properties

The tensile properties of PET fabrics after different treatments are listed in Table 2. In

comparison with the untreated PET fabrics, the tensile strengths of the alkali-etched PET fabrics are significantly reduced by 13.4% in warp direction and 22.9% in weft direction respectively, while their corresponding elongations in warp and weft directions increase about 10%. This is ascribed to the hydrolysis of ester linkage by alkali as well as fabric shrinkage formed during the treatment process. When the PET fabrics are subsequently dyed with Disperse Blue 79 at 130ºC for 60 min, the tensile strengths further decrease in both warp and weft directions and the corresponding elongations change slightly. Both tensile strengths and elongations for the TiO_2 coated and simultaneous hydrothermal-dyeing treated H60 PET fabrics have little difference in both directions from that of PET fabrics solely dyed.

Table 2. The tensile strength of PET fabrics

PET fabrics	Tensile strength (N/m)		Elongation (%)	
	Warp	Weft	Warp	Weft
Untreated	950	925	22.9	21.7
Etched by alkali	823	713	25.8	23.9
Solely dyed	778	691	26.0	24.7
One-step H60	782	688	26.2	24.3

3.4.2 Colour Fastness against UV Light

The effects of irradiation time on the K/S values of both solely dyed PET fabrics and simultaneous hydrothermal-dyeing treated H60 PET fabrics exposure to UV light irradiation are revealed in Figure 8. It is noticed that the K/S values for both PET fabrics decrease gradually with the increase of irradiation time. The K/S values of the H60 PET fabrics are slightly larger than those of the solely dyed PET fabrics after exposure to UV, indicating a good colour fastness to UV light irradiation. The reason is due to the fact that an aggregation layer mixed with TiO_2 particles is coated on PET fabric. The UV light can induce the photo-degradation of organic dyes, the TiO_2 nanoparticles can absorb UV irradiation to a lager extent (Han, & Yu, 2006). As a result, the simultaneous hydrothermal-dyeing treatment for PET fabric can slightly improve the colour fastness to UV light.

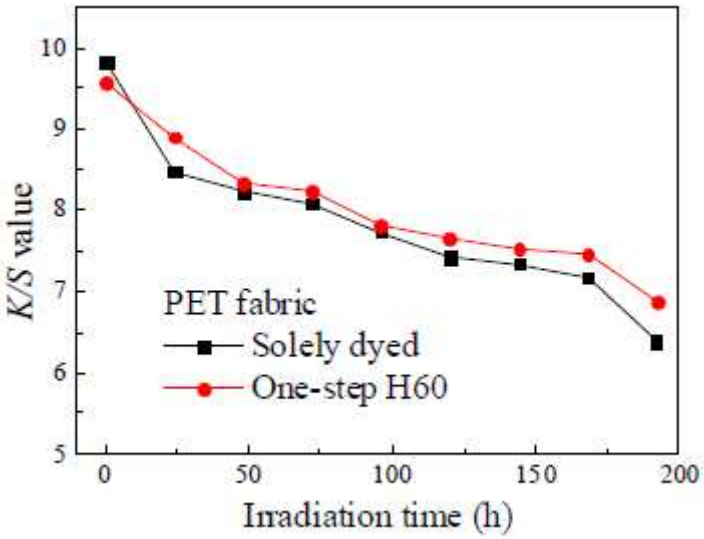

Figure 8. Effects of irradiation time on the K/S values of the solely dyed and simultaneous hydrothermal-dyeing treated H60 PET fabrics exposed to UV light irradiation

3.4.3 Optical Properties

The optical properties of PET fabrics are measured by diffuse reflectance spectra, as illustrated in Figure 9. It is found that the untreated PET fabric can absorb most of UV light irradiation and reflects most of visible light irradiation. Two typical absorption peaks at 226 nm and 304 nm are observed in the untreated PET fabric. This is assigned to the $\pi \rightarrow \pi^*$ electronic transition in benzene ring (Laskarakis, & Logothetidis, 2007). After being coated with a film of TiO_2, the ability to absorb UV and visible light irradiations is enhanced. This is caused by the band gap transition of TiO_2 (Lopez, & Gomez, 2012). As expected, when PET fabric is dyed with Disperse Blue 79, the reflectance curve is totally dominated by the dye used. The reflectance curve of the simultaneous hydrothermal-dyeing treated H60 PET fabric is almost overlapped with that of the solely dyed one. The existence of TiO_2 nanoparticles in the coating has little influence on the optical properties of the H60 PET fabric.

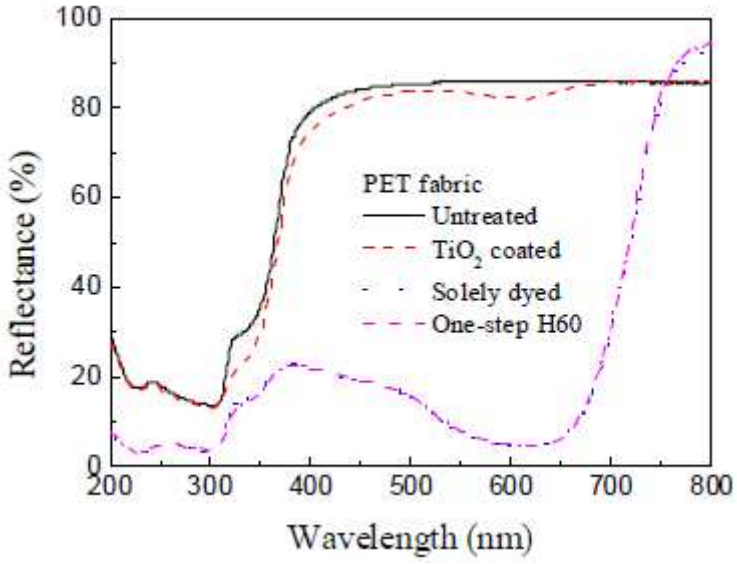

Figure 9. Diffuse reflectance spectra of PET fabrics

3.4.4 Wicking Effect

The dynamic changes of liquor wicking heights with wicking time for the solely dyed and simultaneous hydrothermal-dyeing treated H60 PET fabrics in warp and weft directions are exhibited in Figure 10. The untreated PET fabric has no ability to absorb the deionized water because there is no hydrophilic groups like -OH and -COOH on fabric surface. It is appeared that the liquor wicking heights increase gradually with the increase of wicking time for both fabrics in warp and weft directions, as described in Washburn equation (Darbyshire et al, 1993). Given the same wicking time duration, the wicking heights in warp direction are greater than in weft direction, and the H60 PET fabrics produced from the simultaneous hydrothermal-dyeing processes exhibit greater wicking heights than the solely dyed PET fabrics possibly due to the inherent hydrophilic properties of TiO_2. It is known that greater specific surface area and smaller channels inside textile fabrics leads to greater wicking heights (Li, & Joo, 2012), the greater specific surface area of the H60 PET fabrics is achieved after being deposited with a layer of TiO_2 nanoparticles will result in more rapid upward movement of water along the inter-fiber and inter-yarn capillary spaces (Hashemizad et al, 2012). Additionally, the as-synthesized nanoparticles are coated by a very thin film of hydrophilic organic materials, as demonstrated by TEM, these hydrophilic organic materials could contribute to the greater hydrophilicity and improved wicking performance of the resultant PET fabrics.

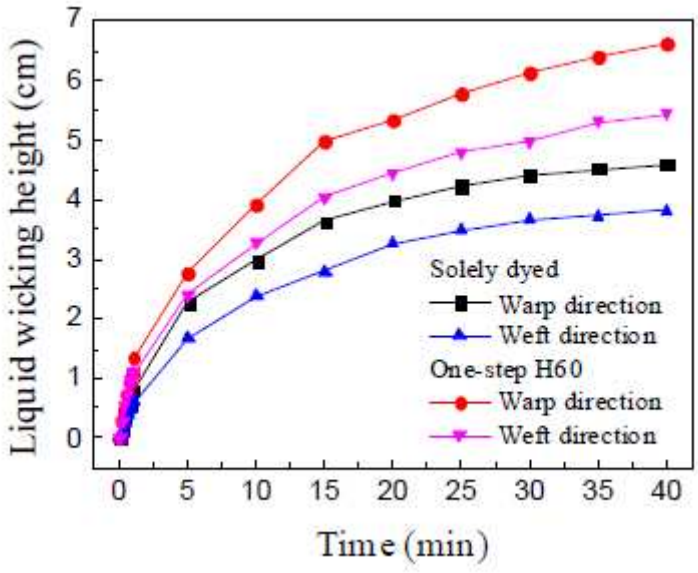

Figure 10. The relationship between liquor wicking height and wicking time for PET fabrics

3.4.5 Percentage of Exhaustion

The relationships between percentages of exhaustion and dyeing temperatures (or dyeing time inserted) of the solely dyed and simultaneous hydrothermal-dyeing treated H60 PET fabrics are disclosed in Figure 11a. For both fabrics, the percentages of exhaustion of Disperse Blue 79 dye increase with the increase of dyeing temperature or dyeing time. Most of dyes are absorbed by PET fabrics when the dyeing temperatures are higher than 120^{o}C or when the dyeing time is beyond 95 min. In the initial dyeing process (dyeing temperature less than 70^{o}C or dyeing time smaller than 45 min), the percentages of exhaustion are very close for both dyeing programs. It means the insoluble dyes are mainly dispersed in the dye bath without interaction between tetrabutyl titanate, PET fabric and dyeing auxiliaries. The percentages of exhaustion for the solely dyed fabrics are larger than those for the simultaneous hydrothermal-dyeing treated H60 ones in the range of dyeing temperature 70^{o}C to 120^{o}C (dyeing time from 45 to 95 min). This may be because the disperse dyes and/or dyeing auxiliaries react with tetrabutyl titanate, which affect the adsorption of dyes on PET fabrics. When the dyeing temperature is kept at 130^{o}C (dyeing time is in the range of 100-170 min), the percentages of exhaustion for the solely dyeing process is slightly larger than those for the simultaneous hydrothermal-dyeing process. At higher temperature (130^{o}C), the thermal agitation induces the structure of PET to become looser and less crystalline. The opening gaps formed in PET fibers make the dye molecules enter into the tightly-packed polymer chains by means of Van-der-Waals and dipole forces (Kim et al, 2005). However,

the deposition of TiO_2 particles on PET fibers may impede the penetrating of dye molecules into the matrix of PET fibers to a certain degree (Zhang et al, 2013). The optical images of dyeing liquors for both fabrics are shown in Figure 11b. The numbers marked in the bottom indicate the dyeing temperature, while the numbers labeled in the upper indicate the corresponding dyeing time. The colours of dyeing liquors for the solely dyeing program change from blue-black to shallow blue as the dyeing temperatures or dyeing time increase. When tetrabutyl titanate is added into the dye bath, the colours of dyeing liquors for the simultaneous hydrothermal-dyeing program are blue with a little red. After centrifugation, the red colours of dyeing liquors become more prominent, especially at low temperature. Meanwhile, some white sediments can be found in the bottom of dyeing liquors.

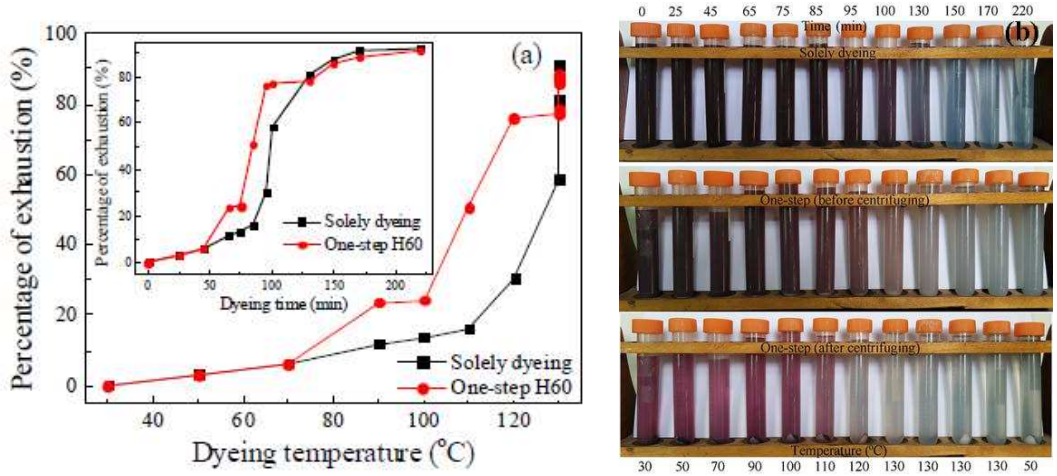

Figure 11. Varying of percentage of exhaustion with dyeing temperature (inserted: varying of percentage of exhaustion with dyeing time) (a) and optical images (b) of dyeing liquors

4. Conclusions

In this work, PET fabrics were dyed using Disperse Blue 79 dye and simultaneously treated with tetrabutyl titanate in a hydrothermal process. It was found that the resultant PET fabrics were covered by a layer of TiO_2 nanoparticles, mixed with a layer of organic dispersion agents. In comparison with the apparent photocatalytic activities of the crystalline TiO_2 particles formed on PET fabrics in solely hydrothermal processes using tetrabutyl titanate, the TiO_2 nanoparticles both formed on the surface of PET fabrics and as-synthesized in the liquid in the simultaneous hydrothermal-dyeing process are non-crystalline and covered with a layer of organic coatings, these TiO_2 nanoparticles do not show any photocatalytic activity. This leads us to believe that the non-crystalline microstructure of the resultant tetrabutyl titanate produced in the simultaneous hydrothermal-dyeing process might be greatly influenced by

the presence of dyestuff and dyeing auxiliaries. However, it is unclear whether the losses of photocatalytic activity of the resultant TiO_2 nanoparticles are due to the thin film of organic substances (from dyestuff and dyeing auxiliaries) covered on the surface of the TiO_2 nanoparticles or caused by the non-crystalline microstructure of the TiO_2 nanoparticles formed.

Acknowledgments

The authors acknowledge the supports from science and technology program (No. 2015049) of China National Textile and Apparel Council and the China Scholarship Council.

References

Awitor , K. 0. , Rivaton , A. , Gardette , J.-L. , Down , A. J. , & Johnson , M. B. (2008). Photo-protection and photo-catalytic activity of crystalline anatase titanium dioxide sputter-coated on polymer films. Thin Solid Films, 516, 2286-2291.

Benmami , M. , Chhor , K. , & Kanaev , A. V. (2006). High photocatalytic activity of monolayer nanocoatings prepared from non-crystalline titanium oxide sol nanoparticles. Chemical Physics Letters, 422, 552-557.

Cho , D. H. (2004). Experimental study on dyeing technical PET yarns having different TiO_2 contents. Fibers and Polymers, 5, 321-326.

Darbyshire , J. F. , Chapman , S. J. , Cheshire , M. V. , Gauld , J. H. , McHardy , W. J. , Paterson , E. , & Vaughan , D. (1993). Methods for the study of interrelationships between micro-organisms and soil structure. Geoderma, 56, 3-23.

Deniz , A. E. , Celebioglu , A. , Kayaci , F. , & Uyar , T. (2011). Electrospun polymeric nanofibrous composites containing TiO_2 short nanofibers. Materials, Chemistry and Physics, 129, 701-704.

EL-Mekkawi , D. M. , Nady , N. , Abdelwahab , N. A. , Mohamed , W. A. A. , & Abdel-Mottaleb , A. S. A. (2016). Flexible bench-scale recirculating flow CPC photoreactor for solar photocatalytic degradation of methylene blue using removable TiO_2 immobilized on PET sheets. International Journal of Photoenergy, 9270492-1-9.

Ghoreishian, S. M., Badii, K., Norouzi, M., & Malek, K. (2016). Effect of cold

plasma pre-treatment on photocatalytic activity of 3D fabric loaded with nano-photocatalysts: Response surface methodology. Applied Surface Science, 365, 252-262.

Ghoreishian , S. M. , Badii , K. , Norouzi , M. , Rashidi , A. , Montazer , M. , Sadeghi , M. , & Vafaee , M. (2014). Decolorization and mineralization of an azo reactive dye using loaded nano-photocatalysts on spacer fabric: Kinetic study and operational factors. Journal of the Taiwan Institute of Chemical Engineers, 45, 2436-2446.

Han , K. Q. , & Yu , M. H. (2006). Study of the preparation and properties of UV-locking fabrics of a PET/TiO_2 nanocomposite prepared by in situ polycondensation. Journal of Applied Polymer Science, 100, 1588-1593.

Hashemizad , S. , Montazer , M. , & Rashidi , A. (2012). Influence of the surface hydrolysis on the functionality of poly(ethylene terephthalate) fabric treated with nanotitanium dioxide. Journal of Applied Polymer Science, 125, 1176-1184.

Kaur , K. , & Singh , C. V. (2012). Amorphous TiO_2 as a photocatalyst for hydrogen production: A DFT study of structural and electronic properties. Energy Procedia, 29, 291-299.

Kim , T. K. , Son , Y. A. , & Lim , Y. J. (2005). Thermodynamic parameters of disperse dyeing on several polyester fibers having different molecular structures. Dyes and Pigments, 67, 229-234.

Laskarakis , A. , & Logothetidis , S. (2007). Study of the electronic and vibrational properties of poly(ethylene terephthalate) and poly(ethylene naphthalate) films. Journal of Applied Physics, 101, 053503-1-9.

Li , Q. S. , Xu , M. S. , Zhou , G. J. , & Wang , L. Q. (2010). Preparation and characterization of white bamboo charcoal PET fiber. Chinese Chemical Letters, 21, 995-998.

Li , Y. , & Joo , C. W. (2012). Pore structure and liquid behavior of nonwovens composed of nanosized fibers by conjugate spinning. Journal of Applied Polymer Science, 126, E252—E259.

Lopez , R. , & G6mez , R. (2012). Band-gap energy estimation from diffuse reflectance measurements on sol-gel and commercial $Ti0_2$: A comparative study. Journal of Sol-Gel Science and Technology, 61,1-7.

Meng , X. F. , Feng , X. Y. , Li , Z. F. , & Zhang , Y. (2012). Fabrication of novel poly (ethylene terephthalate)/TiO_2 nanofibers by electrospinning and their photocatalytic activity. Current Nanoscience, 8, 3-6.

Pandiyaraj , K. N. , Deshmukh , R. R. , Mahendiran , R. , Su , P. G. , Yassitepe , E. Shah , I. , Nadagouda , M. N. (2014). Influence of operating parameters on surface properties of RF glow discharge oxygen plasma treated $Ti0_2$/PET film for biomedical application. Materials Science and Engineering: C, 36, 309-319.

Peng, X. Y., Ding, E. Y., & Xue, F. (2012). In situ synthesis of $Ti0_2$/polyethylene terephthalate hybrid nanocomposites at low temperature. Applied Surface Science, 258, 6564-6570.

Ratova, M. , West , G. T. , & Kelly , P. J. (2014). Optimisation of HiPIMS Photocatalytic titania coatings for low temperature deposition. Surface & Coatings Technology, 250, 7-13.

Rehan , M. , Hartwig , A. , Ott , M. , Gatjen , L. , & Wilken , R. (2013). Enhancement of photocatalytic self-cleaning activity and antimicrobial properties of poly(ethylene terephthalate) fabrics. Surface & Coatings Technology, 219, 50-58.

Sun, Z. G. , Li , X. S. , Zhu , X. B. , Deng , X. Q., Chang, D. L. , & Zhu , A. M. (2014). Facile and fast deposition of amorphous TiO_2 film under atmospheric pressure and at room temperature, and its high photocatalytic activity under UV-C light. Chemical Vapor Deposition, 20, 8-13.

Yang , H. G. , & Zeng , H. C. (2004). Preparation of hollow anatase TiO_2 nanospheres via Ostwald ripening. The Journal of Physical Chemistry B, 108, 3492-3495.

Yu , J. G. , Zhang , L. J. , Cheng , B. , & Su , Y. R. (2007). Hydrothermal preparation and photocatalytic activity of hierarchically sponge-like macro-/mesoporous titania. The Journal of Physical Chemistry C, 111, 10582-10589.

Zhang, F. X., Liang, H., & Zhang, G. X. (2016). Colorant-free coloration and superhydrophilic modification of poly(ethylene terephthalate) fabric surface by H_2O_2 and nano-TiO_2 ultraviolet photocatalysis. Textile Research Journal, 86, 1009–1022.

Zhang, H., Li, F., & Zhu, H. (2013). Immobilization of TiO_2 nanoparticles on PET fabric modified with silane coupling agent by low temperature hydrothermal method. Fibers and Polymers, 14, 43–51.

Zhang, H., Xu, J., & Yang, L. (2011). Modification of PET fabric using tetrabutyl titanate by hydrothermal method. SEN-I GAKKAISHI, 67, 225–231.

Zhang, H., Zhu, H., & Sun, R. J. (2012). Fabrication of photocatalytic TiO_2 nanoparticle film on PET fabric by hydrothermal method. Textile Research Journal, 82, 747–754.

Zhang, P., Wu, C. C., Han, Y. S., Jin, T., Chi, B., Pu, J., & Jian, L. (2012). Low-temperature preparation of hierarchical structure TiO_2 for flexible dye-sensitized solar cell. Journal

of the American Ceramic Society, 95, 1372–1377.

Zou, J., Gao, J., & Xie, F. (2010). An amorphous TiO_2 sol sensitized with H_2O_2 with the enhancement of photocatalytic activity. Journal of Alloys and Compounds, 497, 420–427.